STM studies of PtSi formation on Si(111) by solid state epitaxy

doi: 10.1103/PhysRevB.72.205302

STM studies of PtSi formation on Si(111) by solid state epitaxy

A. Wawro,[1,2,*] S. Suto,[3] and A. Kasuya[1]
[1]*Center for Interdisciplinary Research, Tohoku University, Sendai 980-8578, Japan*
[2]*Institute of Physics, Polish Academy of Sciences, Al. Lotników 32/46, 02-668 Warszawa, Poland*
[3]*Department of Physics, Graduate School of Science, Tohoku University, Sendai 980-8578, Japan*
(Received 6 April 2005; revised manuscript received 19 July 2005; published 3 November 2005)

Formation process and surface structure of platinum silicide thin layers have been studied using scanning tunneling microscopy. The investigated structures have been grown by solid state epitaxy upon deposition of 5 and 10 monolayers (ML) of platinum on the Si(111) surface and annealing at temperatures between 250 °C and 1100 °C. Platinum silicide exhibits a tendency to form islands as the annealing temperature increases. At a coverage of 5 ML the platinum silicide grows epitaxially with the relation of PtSi(010)‖Si(111). In contrast, for 10 ML coverage the PtSi(100)‖Si(111) growth was found. New types of surface reconstruction were observed on the both surfaces. Models successfully explaining investigated reconstructions are proposed. The electronic structure of platinum silicide in the vicinity of the Fermi level has been deduced from the scanning tunneling spectroscopy measurements.

DOI: 10.1103/PhysRevB.72.205302 PACS number(s): 68.35.Bs, 68.37.Ef, 82.65.+r

I. INTRODUCTION

The indirect nature of the silicon energy band gap causes Si technology that lacks the possibility of optical integration. This fact is one of the reasons why in the last years transition-metal and noble-metal silicides have focused considerable attention as a research topic to extend silicon technology for practical applications over new areas. Among numerous metal silicides, platinum silicide seems to offer promising properties. Despite abundance of intermetallic compounds, due to a complexity of Pt-Si phase diagram, three phases: Pt_3Si, Pt_2Si, and PtSi are distinct, however only two latter ones are stable at room temperature.

It has been shown that PtSi/*n*-Si Schottky diodes have one of the highest barriers.[1] On the other hand the barrier height of PtSi/*p*-Si junctions, equal to 220 meV, is the second lowest among known silicides.[2] It well suits for 3–5 μm wavelength range and makes these heterostructures one of the most successful for photoemissive infrared detectors.[2–7] Low resistivity and thermal stability are the properties, which favour metal silicides for Ohmic contacts in silicon based semiconductor technology. Titanium disilicide ($TiSi_2$) is one of the most widely utilized materials for this purpose. However, when the one of its lateral dimensions shrinks to submicron range, the resistance increases drastically.[8,9] Platinum silicide is a good candidate to overcome this problem, because it offers low and stable resistance also in nanometer scale.[10] The use of platinum silicide layers as a component of grazing incidence mirrors for x-ray beam is another challenge for practical application.[11]

For the sake of application in electronic devices, where the thin film technology dominates, the initial stage of platinum silicide formation process on the silicon surface is a subject of particular interest. Although reactions between deposited platinum and the silicon substrate have been widely studied, the details of processes occurring at the interface are still discussible. At the initial stage of deposition at room temperature Pt atoms do not diffuse into Si bulk, forming a monolayer thick metallic coverage.[12–14] However, the signs of the reaction appear after the completion of the first monolayer.[12] A contrary conclusion that mixing at the interface takes place immediately after the deposition process even for submonolayer amounts has been drawn in Refs. 15 and 16. Low coverage of 0.07 ML of Pt introduces strong modifications in photoemission spectra due to mixing occurring at the interface.[17] Another suggestion states that Pt atoms most probably chemisorb at the sixfold interstitial positions located between the top and the second Si(111) plane, giving rise to complicated distribution of strains in the lattice.[18] With an increasing amount of Pt the elastic energy activates diffusion of Pt atoms into Si bulk. In the case of thicker coverages an intermixing at the interface is frequently reported.[18–22] For thick enough deposited Pt layers the evidence of pure metal existence has been presented.[15,16,20,23,24]

Formation of platinum silicide phase has been inferred from the core and valence electron energy shifts in the component elements detected by means of photoemission spectroscopy (PES),[11,15–17,20,25–29] from extended x-ray absorption fine structure (EXAFS),[18,30] as well as from chemical profile investigations by Rutheford backscattering (RBS),[31,32] Auger electron spectroscopy (AES),[33] transmission electron microscopy (TEM),[29,31] and ellipsometry.[20,34,35] The kinetics of the proceeding reactions is affected by various factors. On the single crystal substrate platinum silicide compounds grow sequentially as the temperature increases. Although various reaction temperatures have been reported, a general conclusion might be drawn that Pt_2Si phase grows between 210 °C and 280 °C (Refs. 20, 28, 29, 31, 34, 36, and 37) due to diffusion of Pt atoms into Si bulk. It proceeds until Pt atoms are entirely exhausted. Above 300–350 °C formation of PtSi phase takes place starting from the interface between Pt_2Si and Si by in-diffusion of Si atoms into Pt_2Si lattice. Both processes are diffusion limited,[31] however they proceed rapidly.[29] Time necessary for Pt_2Si growth at 300 °C is of the order of single seconds, whereas complete silicidation to PtSi phase occurs within 2 min.[29] Ellipsometry

studies of kinetic parameters reveal activation energies of 1.50 eV and 1.70 eV and reaction coefficients of 37 cm^2/s and 27 cm^2/s for a transition of Pt to Pt_2Si and Pt_2Si to PtSi, respectively.[34,35] Several models of the interface structure, formed during reaction between Pt and Si, have been proposed.[16,29,34,35,38] Although chemical composition of silicide film is reported to be in general homogeneous, the appearance of segregation in the form of PtSi clusters[36] and columns of PtSi phase in Si matrix[32] has been also revealed. As already mentioned above, the growth of platinum silicide phases is sequential. However in the case of an amorphous silicon substrate[39] or in the presence of oxygen in the grown layers[29,40,41] Pt_2Si and PtSi phases may coexist.[42,43] Platinum silicide films grown at low temperature range are smooth and continuous.[36] As the temperature of thermal treatment increases a transition from the smooth to islandlike structure is reported. It results in degradation of surface quality as well as in increase of sheet resistivity.[33] Observed tendency has been explained by intensive diffusion of Pt atoms from PtSi/Si interface into Si bulk due to the low eutectic point at 830 °C.[33,44] Implantation of fluorine atoms eliminates platinum silicide surface degradation. Segregated at the silicide-silicon interface, most probably due to high Si-F binding energy, they prevent the transport of Pt atoms into Si substrate even at 800 °C, considerably improving high temperature stability of PtSi films.[33]

Despite numerous investigations by means of techniques, which average the properties of platinum silicide layers over a large probed area, the studies of local properties and morphology in nanometer scale are rather limited. The aim of this work is to complete and expand the knowledge on thin film platinum silicide evolution upon low coverage deposition of platinum (5 and 10 ML) and subsequent thermal treatment between room temperature and 1100 °C. Applied ultrahigh vacuum scanning tunneling microscopy (UHV STM) is an ideal tool, which enables us to study the surface morphology of grown platinum silicides in a real space with the resolution of interatomic distances. Additionally, by means of scanning tunneling spectroscopy (STS), it provides probing possibilities of a local electronic structure in the vicinity of the Fermi level. Such detailed insight is particularly important for proceeding miniaturization of platinum silicide based devices when their lateral dimensions shrink into several nanometers and local fluctuations start to play a significant role.

II. EXPERIMENT

Experiments were performed in an UHV system, which consisted of analysis chamber and a sample preparation chamber. The analysis chamber was equipped with a STM (VT-STM, Omicron) and an electron beam evaporator (EFM3, Omicron). The evaporator was mounted at oblique incidence position. The base pressure of the analysis chamber was in the low range of 10^{-10} Torr and below 5×10^{-10} Torr during deposition. Commercial *n*-type Si(111) wafers (phosphorus doped, ~3 Ω cm), cut to bars approximately $9\times1\times0.5$ mm^3 in size, were used as the substrates. In order to get a clean Si(111)7×7 surface, the substrates were heated resistively at 700 °C for several hours by directly flowing current followed by flashing at 1250 °C in the preparation chamber. Then they were cooled down to room temperature at the rate lower than 1 °C/s. Consequently, the high quality of the 7×7 reconstruction with negligible amount of defects and contaminations on the surface was reproducibly obtained. The platinum was evaporated from the electron gun at a rate lower than 1 ML/min onto the substrate kept at room temperature. A flux and a total amount of deposited metal were measured by a flux monitor integrated with the evaporator. The STM measurements were performed at room temperature after platinum deposition and subsequent annealing at consecutive temperatures: 250 °C, 400 °C, 550 °C, 750 °C, 950 °C, and 1100 °C. At each temperature samples were kept for 10 min and cooled down spontaneously after rapid cutting off a heating current. Tungsten STM tips were electrochemically etched and cleaned by annealing in the vacuum system. Then the bias pulses were applied between tip and dummy sample. At positive voltage the empty states of the sample were probed whereas for negative bias—the filled ones. All topography images were recorded in the constant current mode.

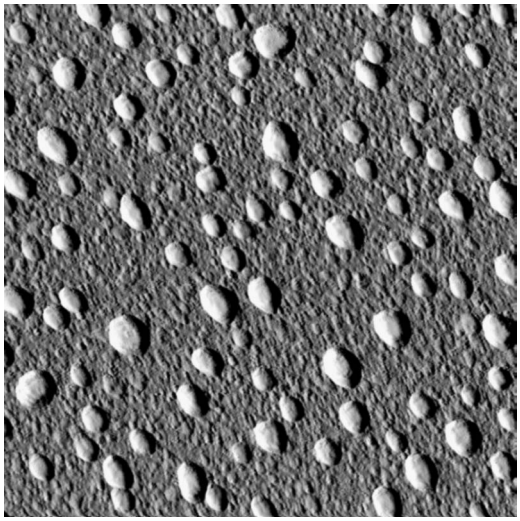

FIG. 1. Derivative STM image (200 nm × 200 nm) of platinum silicide islands formed after deposition of 5 ML Pt and annealing at 400 °C.

III. RESULTS

A. Deposition of 5 ML Pt

At the room temperature, no STM image with atomic resolution is observed although the modified α-7×7 or $\sqrt{7}\times\sqrt{7}$ reconstructions have been detected by the LEED.[13,45,46] The surface morphology is uniform in the micrometer scale. A grainy structure of 0.3 nm in corrugation and 3 nm in diameter is observed in the nanometer scale. At 250 °C annealing, the grains grow bigger reaching the size of 0.8 nm in corrugation and 7 nm in diameter.

At 400 °C annealing, we observe the substantial changes in growth mode. Figure 1 shows the STM image of randomly distributed islands with different sizes. The biggest islands

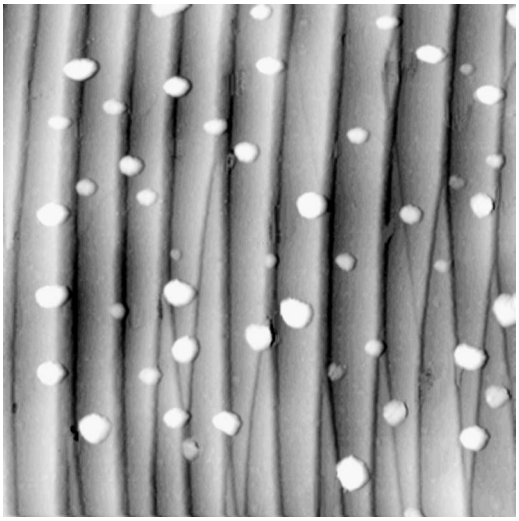

FIG. 2. Platinum silicide islands grown upon deposition of 5 ML Pt and annealing at 550 °C. The size of STM image: 1000 nm × 1000 nm.

reach the size of 2 nm in height and 15 nm in diameter, whereas the smallest are the two times as small as the biggest ones. The steps of the substrate surface do not influence the position of islands. At 550 °C annealing, the islands size becomes bigger and approaches 10 nm in height and 30 nm in diameter as shown in Fig. 2. The density of islands reduces from 2000 to 40 per square micrometer. A reconstruction of island surfaces is getting distinct. About the half of islands has a well developed the reconstruction, which becomes clearer at 750 °C annealing.

At 750 °C annealing, Fig. 3 exhibits only one island in the area of square micrometer and the size of the island enlarges up to 8 nm in height and 100 nm in diameter. The islands take more regular shapes determined by the platinum silicide crystal structure symmetry. The details of reconstructed surface are displayed in Fig. 4. The topmost atoms are arranged in triangles with truncated vertices. Each side of

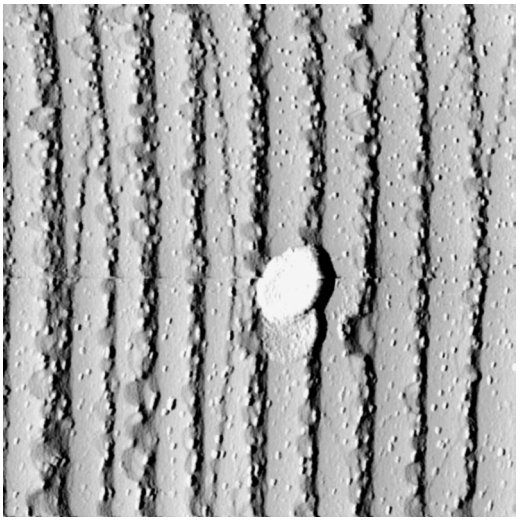

FIG. 3. Single PtSi island formed after deposition of 5 ML Pt and annealing at 750 °C. The scan size: 1000 nm × 1000 nm.

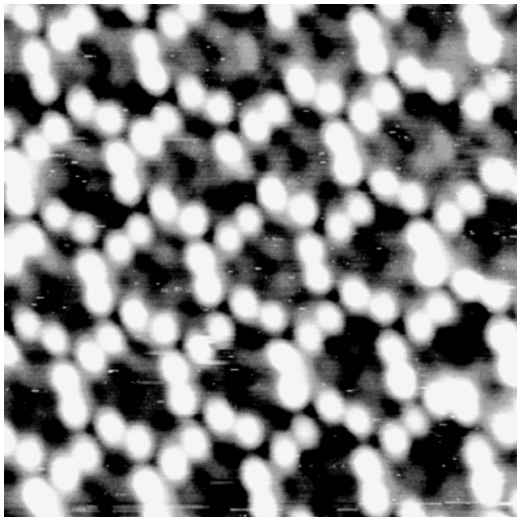

FIG. 4. The details (10 nm × 10 nm) of the island surface reconstruction formed after deposition of 5 ML Pt and annealing at 750 °C. Apart from the reconstruction atoms the structural features of the underneath layer are visible.

the triangle consists four atoms. Two center ones are brought slightly closer, suggesting a tendency to form dimers. The distance between outer and central atoms exceeds 0.7 nm, whereas the distance between two central atoms is smaller than 0.6 nm. The shape of the triangles is slightly stretched along a diagonal from upper left towards bottom right corner. Moreover, three weak protrusions 0.03 nm in height appear near the vertices inside of each triangle. The reconstruction extends over the whole island surface and no structural domains are found. The STM images do not depend on the bias voltage and the sign.

B. Deposition of 10 ML Pt

Above 250 °C annealing, the islands grow with a different mode from the case of 5 ML. A prevailing parts of the sample surface are not well ordered, but small parts display a regular alignment of atoms at 250 °C annealing. Figure 5 shows the STM image of the ordered area. The distance between atoms and the surface structure are the same as these of $\sqrt{3} \times \sqrt{3}$ reconstruction of a Si(111) surface.

A mosaiclike structure shows up at 400 °C annealing and covers uniformly the sample surface at 550 °C annealing as shown in Fig. 6. Component tiles, about 70 nm in diameter have nonregular shapes. Figure 7 shows the STM image at 750 °C annealing. The proceeding reaction results in nonuniform surface morphology and the island grows 5 nm in height. The mosaiclike structure of the island surface with the same size of constituent tiles is still maintained but the island area is reduced to approximately a half of the surface. Structural domains are rotated by 60° each other and a bricklike structure is distinguished in individual tiles as shown in Fig. 8. This observation confirms the epitaxial growth of the islands on a Si(111) surface.

The details of reconstruction structure are shown in Fig. 9. The bricklike elements are very regularly aligned and expand over the distance of several tens of nanometers. The

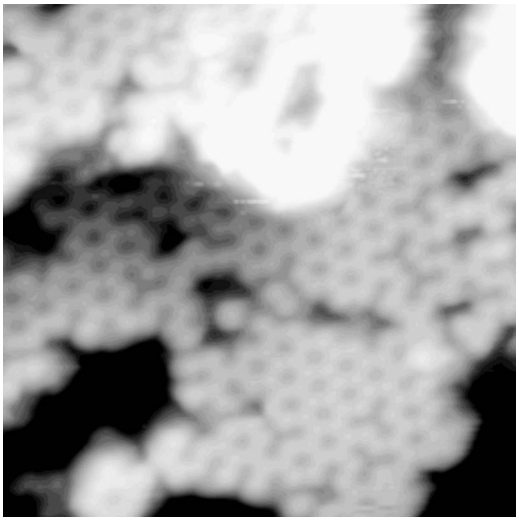

FIG. 5. Surface reconstruction observed upon deposition of 10 ML Pt and annealing at 250 °C. The image scan size: 11.7 nm $\times$ 11.7 nm.

topmost atoms of individual bricks are arranged in two parallel rows shifted by half of an interatomic distance, forming a zig-zag structure. Along the row, the atoms are separated by 0.39 nm. A distance between nearest neighbors in adjacent rows is slightly larger and equal to 0.42 nm. Each row consists mostly of 4 or 5 atoms. A histogram with a well pronounced maximum shown in Fig. 10 reflects the uniformity of the brick size. The bricks of the smallest size appear as defects inside of the well defined net, whereas largest elements are encountered usually in the vicinity of tile boundaries. In a direction perpendicular to the longer axis of the bricks they are aligned in a ladderlike structure with distance between them equal to 1.16 nm. Adjacent ladders are shifted by half of this distance. Individual atoms of the bricks are imaged in the same way and their corrugation, measured by STM, equal to 0.08 nm, does not depend on the value and

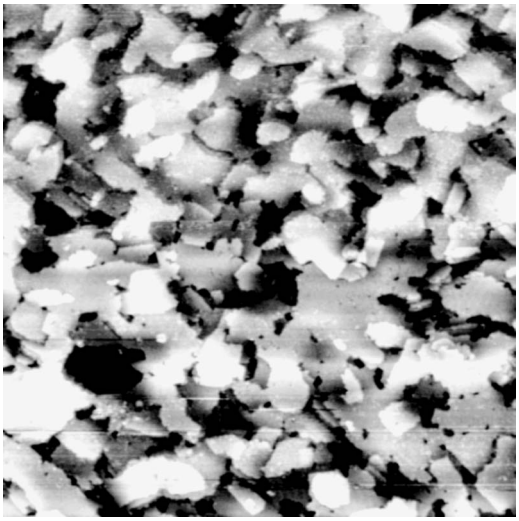

FIG. 6. Mosaiclike structure of PtSi layer grown upon deposition of 10 ML Pt and annealing at 550 °C. The size of STM image: 300 nm $\times$ 300 nm.

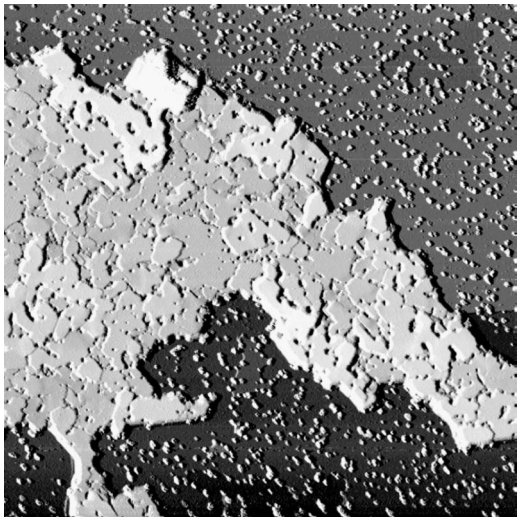

FIG. 7. The islandlike growth of PtSi crystallized after deposition of 10 ML Pt and annealing at 750 °C. PtSi island is surrounded by the fully reacted area. The size of STM image: 1000 nm $\times$ 1000 nm.

sign of the applied bias. Such behavior suggests the same type of constituent atoms of reconstruction and metallic nature of probed orbitals. Thus the character of terminating atoms is similar in two observed reconstructions.

C. A $\sqrt{3}\times\sqrt{3}$ reconstruction between islands

For both coverages of Pt at annealing above 550 °C a $\sqrt{3}\times\sqrt{3}$ ordered surface expands between islands of platinum silicide. Above 950 °C annealing this reconstruction is only found on the sample surface. Figures 11(a) and 11(b) show STM images of a $\sqrt{3}\times\sqrt{3}$ ordered surface after annealing at 1100 °C. The topmost atoms, spaced by the distance of 0.66 nm, are arranged in a close packed structure contain-

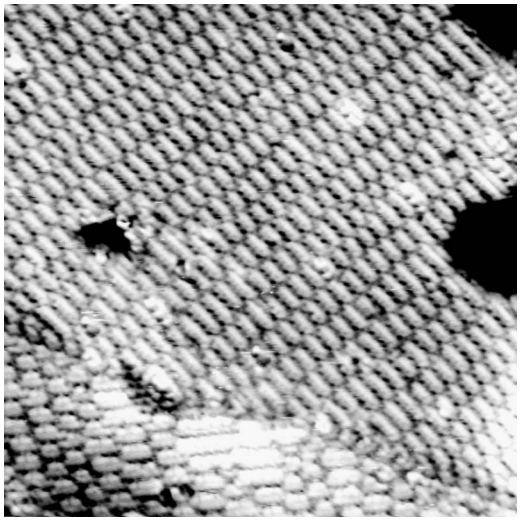

FIG. 8. Details of mosaic pattern formed upon deposition of 10 ML Pt and annealing at 750 °C. Two structural domains rotated by 60° are clearly visible. The size of STM image: 35 nm $\times$ 35 nm.

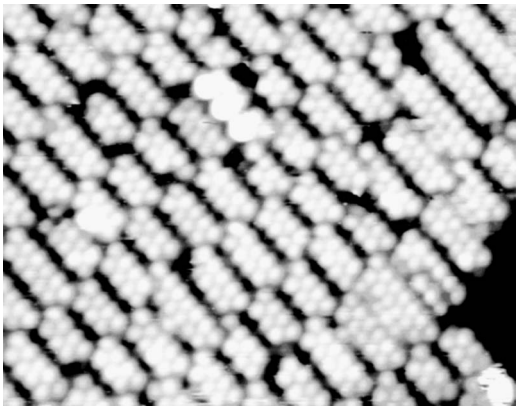

FIG. 9. A bricklike reconstruction of PtSi surface formed after deposition of 10 ML and annealing at 750 °C. The size of STM image: 15 nm × 11.8 nm.

ing the relatively high density of linear defects. As a consequence the surface structure consists of structural domains several nanometers in size, separated by the boundaries. Although all surface atoms inside of the individual domains are imaged in the same way at various gap voltages, the boundary atoms exhibit a bias dependent nature as shown in Fig. 11(b). The borders are imaged as herringbone patches, when the empty states of the sample are probed. Their apparent height, measured relatively to unchanged corrugation inside the domains, is equal to 0.05 nm. Observed structures are very well localized and constrained only to the atoms forming the boundaries. Their neighborhood does not affect the imaging of atoms belonging to the domain interior. Presented features are highly reproducible: after switching the bias from negative to positive value and vice versa, the protruded structures of domain boundaries disappear and appear again, respectively. Their orientation is imposed by the substrate symmetry and equally encountered along all three equivalent directions, rotated every 60°. Additionally, the observed structures are very stable. Numerous subsequent annealing at

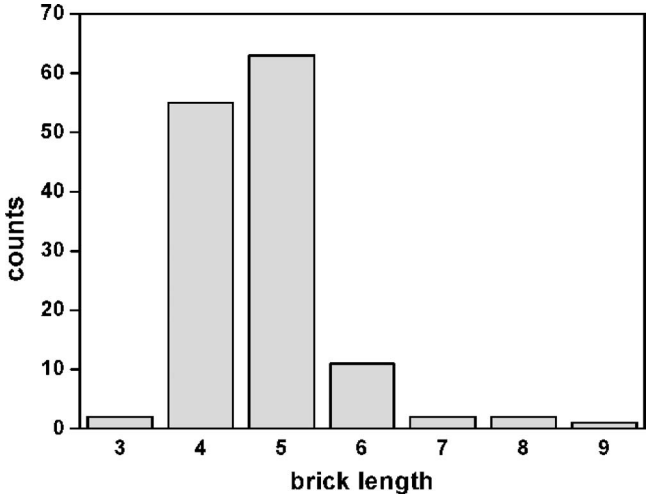

FIG. 10. A histogram of brick sizes measured as a number of atoms in a single row. The length uniformity for 4 and 5 atoms is very high.

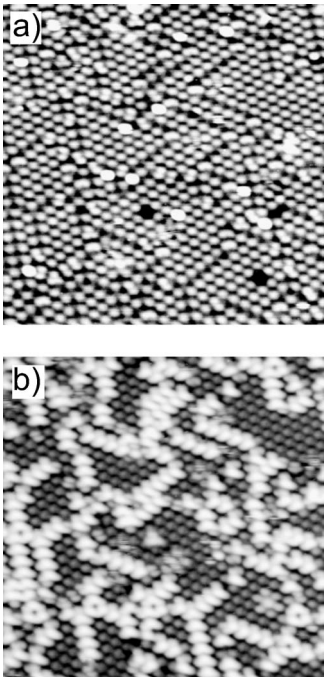

FIG. 11. The $\sqrt{3} \times \sqrt{3}$ reconstruction after annealing at 1100 °C. The STM images show the same area (20 nm × 20 nm) recorded at two various biases: (a) −1.19 V and (b) 1.19 V. The domain boundaries are imaged as "herringbone" protrusions for empty states.

various temperatures, lower than 1100 °C, various duration and different cooling rates down to room temperature, do not change them noticeably.

IV. DISCUSSION

A. Formation process of the platinum silicide islands

A comparison of our results with available in the literature data allows to identify reactions occurring on the surface upon Pt deposition and subsequent annealing. The lack of long range ordering and grainy topography observed after Pt deposition at room temperature and at 250 °C annealing suggests that silicidation process is not completed yet below this temperature. It should be expected that intermixing takes place at the Pt/Si interface and a development of crystallized platinum silicide structure requires a higher temperature. The coexistence of reconstructed and unreconstructed surface, shown in Fig. 5, indicates that the reactions of deposited Pt occur with the Si substrate. However the reaction proceeds nonuniformly across the Si surface. Most likely the Pt_2Si phase is crystallized in the area covered with reconstructed surface, because the temperature of 250 °C is too low for PtSi phase formation.

We suppose that after annealing at 400 °C a well crystallized silicon-rich phase PtSi is already present for both Pt coverages. For the sample covered with 5 ML of Pt the islands persist up to 750 °C. Stable surface reconstruction provides evidence that both the phase and its crystallographic orientation is maintained and any structural crossover does not take place.

Similar conclusions might be drawn for the sample with 10 ML coverage of Pt, although a different reconstruction pattern is observed. This suggests that the growth orientation of platinum silicide thin films is different and thus depends on the amount of initially deposited Pt. Also in this case the reconstruction surface is maintained proving stability of the phase and orientation of platinum silicide up to the temperature of 950 °C.

Predisposition to form islands is a consequence of nonuniform reaction of platinum silicide layer with the substrate proceeding upon annealing. The decrease of the fraction sample surface covered with islands with increasing temperature is a common feature observed for both amounts of deposited Pt. In flat area between PtSi islands, terminated with $\sqrt{3}\times\sqrt{3}$ pattern, which expands with increasing temperature, the intensity of occurring reactions is higher. The atoms of deposited Pt entirely diffuse into Si bulk modifying merely the sample surface.

Observed reconstructions of platinum silicide surfaces are new and to our knowledge not reported in the literature yet. The proposed models are discussed in the next section of our paper. Available results on platinum silicide surface structure, achieved by other groups, are obtained mainly from low energy electron diffraction technique (LEED),[13,14,19,23,45,46] which averages a signal over a relatively large probed area. In general, upon deposition of the Pt amount comparable to our experiment, the 7×7 structure typical of the clean Si(111) surface is modified into α-7×7 and after moderate annealing evolves into $\sqrt{7}\times\sqrt{7}$ pattern. As annealing temperature increases the $\sqrt{3}\times\sqrt{3}$ arrangement is formed, finally followed by 1×1 reconstruction.

B. Models of platinum silicide reconstruction

Our considerations, leading to an explanation of observed reconstructions, are limited only to two stable at room temperature phases: Pt_2Si and PtSi. The Pt_2Si phase crystallizes in the body centered tetragonal lattice. The central Si atom is surrounded by eight Pt atoms located along the symmetry axis of the cell side walls. These Pt atoms sit inside of the tetrahedron determined by four Si atoms. The lattice resembles a CaF_2 structure with a space group $I4/mmm$. (No. 139).[47] The lattice parameters a and c are equal to 0.392 nm and 0.596 nm, respectively. The PtSi phase, also stable at room temperature, has more complicated primitive orthorhombic MnP-type structure with four equivalent Pt and four equivalent Si atoms per cell.[47,48] The space group of this structure is *Pnma* (No. 62).[47] The exact values of atom coordinates along a and c axes are specified in Ref. 48. The lattice parameters a, b, and c are equal to 0.561 nm, 0.359 nm, and 0.593 nm, respectively.

In order to identify the orientation of grown platinum silicide layer and explain the observed surface reconstructions, we have considered arrangements in all low-index planes of type (100), (110), and (111) both of Pt_2Si and PtSi phases and fitted to the structures shown in Figs. 4 and 9. Only the geometrical relations are taken into account and reasonably low lattice mismatch at the interface is accepted. Observed reconstructions of the surface should have the symmetry of the nonreconstructed bulklike atomic plane of the silicide phase. The azimuthal orientation of platinum silicide reconstruction, relative to the $\sqrt{3}\times\sqrt{3}$ structure of the area, which surrounds platinum silicide islands, allows us to determine the crystallographic dependencies between platinum silicide lattice and silicon substrate at the interface.

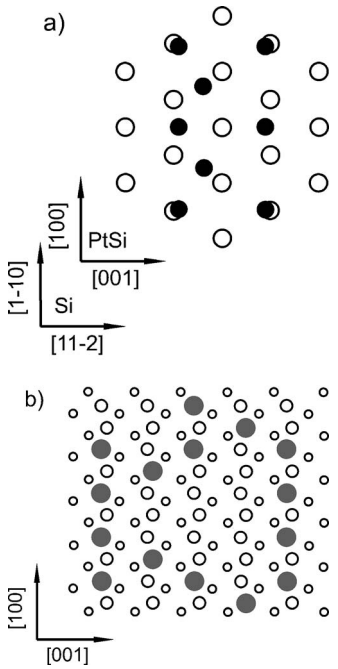

FIG. 12. A model for epitaxial growth of PtSi(010) on Si (111). (a) Azimuthal relations at the Si(111)/PtSi(010) interface. Si atoms of the topmost substrate surface (open circles) bind Si atoms of PtSi crystal (closed circles). (b) The topmost nonreconstructed PtSi(010) surface consist of Si atoms (small open circle) and Pt atoms (big open circles). Reconstruction atoms (gray circles) decorate a part of the Pt atoms of the topmost layer.

The presence of the PtSi phase has been identified for both amounts of deposited Pt. The growth orientations depend on the Pt initial coverage and fulfill the following relations: PtSi(010)‖Si(111) and PtSi(100)‖Si(111), respectively, for 5 and 10 ML of evaporated Pt. The former growth mode has been already discussed in Refs. 19, 32, and 49. Another crystallographic interface relation PtSi(101)‖Si(111) has been also reported,[36] but we did not observe it in our experiment.

1. Coverage of 5 ML

A schematic drawing of a mutual orientation of the Si(111) substrate and PtSi(010) crystallite at 5 ML Pt coverage is shown in Fig. 12(a). The atoms of the unreconstructed Si(111)1×1 surface are aligned in the hexagonal net with a distance of 0.384 nm between nearest neighbors. The PtSi lattice consists of a stack of crystallographically equivalent planes, which contain both Pt and Si atoms. For this growth mode, the direction [11-2] of the Si substrate is parallel to [001] of the PtSi phase. Along these directions every Si atom from the substrate (0.665 nm) fits to the Si atom in the PtSi lattice (0.593 nm). In the perpendicular direction triple dis-

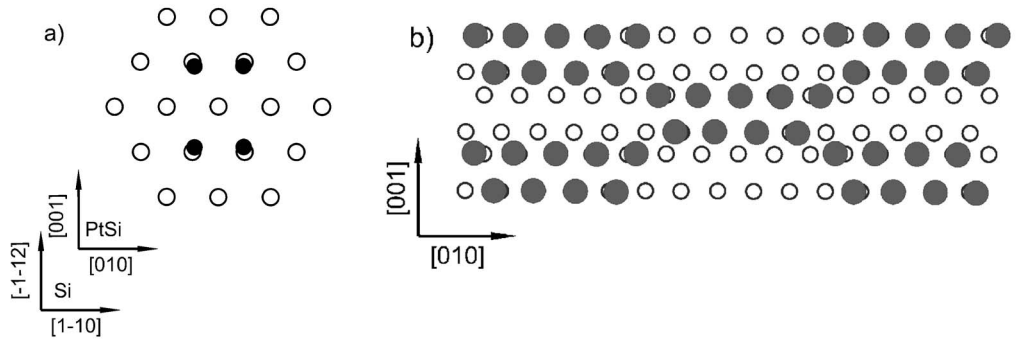

FIG. 13. A model for epitaxial growth of PtSi(100) on Si(111). (a) The structure of Si(111)/PtSi(100) interface. The atoms of silicon substrate (open circles) bind the Si atoms form platinum silicide crystal (closed circles). (b) Bricklike reconstruction of PtSi(100) surface. Reconstruction atoms (gray circles) sit on Pt atoms (open circles) in the topmost layer of PtSi.

tance between substrate atoms (1.152 nm) corresponds to the double one (1.122 nm) in PtSi. Such alignment induces the tensile stresses in the PtSi crystal due to the mismatch between PtSi and Si lattices equal to −10.8% and −2.6% along the [001] and [100] directions of PtSi, respectively. Although the lattice mismatch at the interface is rather large, the epitaxial growth of the PtSi phase on the Si(111) surface is evident. Since the PtSi phase takes shape of islands 100 nm in diameter, as shown in Fig. 3, the presence of dislocations most probably relaxes induced strains and the structure of grown crystallite is monodomain. Moreover the thickness of 8 nm is large enough to obtain a completely relaxed surface of islands.

Figure 12(b) denotes the schematic drawing of the alignment of reconstructed surface atoms. The topmost atoms sit on Pt atoms in the first PtSi layer. The sides of truncated triangles run in [100], [-10-2], and [10-2] directions of the PtSi crystal. Along the [100] direction the atoms are spaced with the same distance equal to 0.561 nm. In the two latter directions, the distance between central atoms is equal to 0.593 nm, whereas the outer atoms are located 0.719 nm away from the central ones. Such reconstruction results in a nonuniform shape of truncated triangles. One of the triangle heights along [001] is larger than two others and they are equal to 2.37 nm and 2.06 nm, respectively. This model reproduces the stretching in one direction as is observed along a diagonal in Fig. 4. Thus, the simple consideration of the PtSi bulk cut along the (010) plane precisely explains the structure observed by STM.

The surface reconstruction has relatively low density of atoms, large periodicity, and a large mesh size. As mentioned earlier reconstruction atoms are located on Pt ones in the topmost layer of the PtSi phase. Numerous Pt and Si atoms in the topmost bulklike plane, which sit inside every mesh, are not imaged individually by STM. Instead the three bumps 0.03 nm in height are visible near the vertices of triangle mesh, but their origin is not clear. It has been recently shown that in the PtSi phase Pt 5*d* orbitals are not highly localized. They extend through the whole valence band.[15,16] An intensive mixing of Pt 5*d* and Pt 6*p* orbitals with Si 3*d* and Si 3*p* ones, a small charge net transfer from Si atom to Pt atom,[16,30] and the existence of three-center Pt-Si-Pt and two-center Pt-Si covalent bonds,[47] additionally in presence of the surface, may cause such complex PtSi electronic structure. The complementary studies with the use of different techniques supported by theoretical considerations are necessary to explain fully the nature of observed surface structure.

2. Coverage of 10 ML

Entirely different PtSi growth mode is found at 10 ML Pt deposition. The surface shows a very regular long range pattern as indicated in Fig. 9. Every constituent bricklike element consists of two rows of atoms. The observed reconstruction is explained in the best way under the assumption that the PtSi phase grows in the (100) orientation. For this orientation the crystalline lattice is built of Pt planes altered with two Si planes. In the Pt plane the atoms form a zig-zag pattern along the [010] direction. The atom arrangement in the Si plane exhibits a rectangular symmetry. The adjacent three-layer slabs are rotated by 180°.

The mutual orientation of the topmost Si(111)1×1 layer and Si layer of PtSi phase is shown schematically in Fig. 13(a). Directions [1-10] and [11-2] of the Si substrate are parallel to [010] and [00-1] in PtSi, respectively. Such alignment induces tensile strains in PtSi due to lattice mismatch equal to −6.5% and −10.8%. This misfit is larger than discussed for PtSi grown upon deposition of 5 ML. It might result here in the multidomain and mosaic structure of silicide, as observed in our experiment, in order to release appearing at the interface strains and lower an elastic component of the energy.

The topmost PtSi layer, consisting of Pt atoms, and the reconstruction atoms are schematically shown in Fig. 13(b). It is plausible that the strains generated at the interface relax through the thickness of the PtSi crystallite and the distances between the atoms in the topmost nonreconstructed plane are bulklike. The distance between Pt atoms along the rows in the [010] direction is equal to 0.359 nm, whereas periodicity in the perpendicular direction [001] is equal to 0.593 nm. As in the case for 5 ML, the symmetry of reconstruction fits to that of Pt in the nonreconstructed topmost plane. The reconstruction atoms are not aligned in long rows. Instead they form very homogeneous in size bricks as depicted in Fig. 10. Two values of the length equal to 4 and 5 atoms in a row are dominating. The carefully measured distance between reconstruction atoms along a row in the individual brick yields a

value of 0.39 nm, which is larger by 9% than that between Pt atoms in bulk PtSi. Therefore the alignment of reconstruction atoms in continuous rows is unfavourable due to the substantial misfit with the layer underneath. To minimize strain energy the reconstruction atoms show a preference to form a brick structure as shown schematically in Fig. 13(b). A very high homogeneity in brick size is a strong argument in explanation of observed reconstruction in terms of the energy elastic driven mechanism. Along the [001] direction the bricks sit on every second zig-zag row of Pt atoms in the topmost bulklike plane. The periodicity is equal to 1.19 nm. This model fits very well to experimentally observed structure shown in Fig. 9.

The lack of bias dependent imaging of atoms constituting two discussed reconstructions for 5 and 10 ML suggests a metalliclike character of their electronic states. Both empty and occupied states are present and there is no spatial shift between them. Despite this finding it is not possible to adjudicate whether Pt atoms or Si form observed structure. Most probably they are Si ones and sit on Pt atoms from the topmost complete layer of PtSi. A strong segregation should not be observed close to the surface due to nearly the same strength of Si-Si and Pt-Si bonds in PtSi.[17,47]

For a first sight it might be surprising that a relatively small difference in the amount of deposited material can result in various modes of PtSi growth. It may be better understood, if the performed experiment is considered as consisting of many steps. As mentioned in the Experiment, to perform the STM investigation, the samples were cooled down to room temperature after annealing at every temperature. A temperature of 250 °C is too low to form the PtSi compound. At this temperature the silicidation process is not completed yet. However due to various coverages, two different chemical composition profiles, induced strains, etc., are plausibly achieved near the interface for both Pt coverages after annealing at 250 °C and cooling down to room temperature. Thus the different starting conditions before annealing at 400 °C, high enough to form PtSi phase, may result in various growth modes of platinum silicide.

C. Reconstruction $\sqrt{3}\times\sqrt{3}$ between islands

In the wide range of high temperatures a flat area, with $\sqrt{3}\times\sqrt{3}$ structure, fills the space between PtSi islands. It is only reconstruction found on the surface above 750 °C and 950 °C for 5 and 10 ML of Pt, respectively. Usually such reconstruction is observed after deposition of 1/3 ML of Pt.[13] One of the models proposes that dispersed metal atoms are ordered near the surface in the sixfold interstitial sites.[46] In our experiment the amount of deposited Pt is much higher that 1/3 ML. We identify the area with $\sqrt{3}\times\sqrt{3}$ reconstruction as places where reaction occurs more rapidly and all deposited Pt atoms diffuse entirely into Si bulk, merely modifying the structure of the surface.

A uniform STM imaging of atoms inside of structural surface domains suggests that all are of the same type. A strong segregation near the surface should not be expected due to comparable strength of Si-Si and Pt-Si bonds.[17,47] The observed $\sqrt{3}\times\sqrt{3}$ reconstruction suggests that only one layer of reconstruction atoms terminates a bulklike Si substrate. Thus those atoms are rather Pt ones than Si. On the contrary, the atoms from the structural domain boundaries are imaged in different way, when the bias switches from negative to positive and in opposite. Such behavior is ascribed to different spatial distribution of occupied and empty states. The same symmetry of patches running along three equivalent directions in various samples excludes artifacts originating from the tip. The modification of unoccupied orbitals is very local and is constrained only to boundary atoms. The observed herringbone structure suggests a strong orbital hybridization of atoms from the domain boundary and the atoms located along the boundary in the layer underneath.

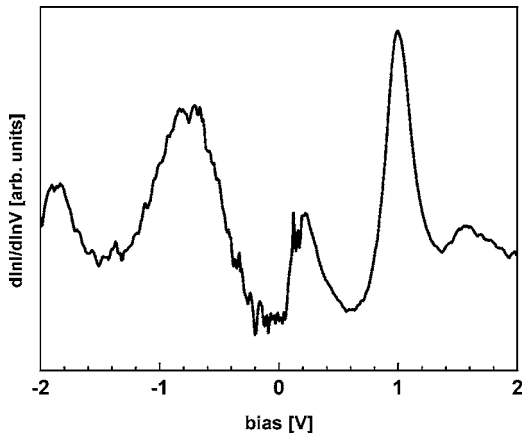

FIG. 14. Logarithmic conductivity d ln I/d ln V measured on the PtSi(100) surface.

D. Spectroscopy

The electronic structure of the PtSi(100) phase is investigated in the vicinity of the Fermi level by scanning tunneling spectroscopy (STS). The bias dependent logarithmic conductivity, which is related to the local density of electronic states, is shown in Fig. 14. The logarithmic conductivity eliminates the influence of varying barrier height with sweeping bias. The low conductivity at 0 V, corresponding to the Fermi level and four peaks at the biases of −1.8 V, −0.8 V, 0.2 V, and 1.0 V are very distinct. The low conductivity at 0 V confirms that PtSi phase is a poor metal with low density of states (DOS) at the Fermi level. This result agrees well with the calculations performed by Beckstein *et al.*[48] and Franco *et al.*[15,16] The peak positions also fit well to mentioned calculations, which lead to the conclusion that the Pt 5*d* orbital is not highly localized. It expands through the whole valence band and is strongly mixed mainly with Pt 6*p*, Si 3*s*, and Si 3*p* states in various extents at different energies. The behavior results in a complex nature of chemical bonds in PtSi compound. On the basis of mentioned theoretical considerations the identification of the observed peaks might be as the following. Strongly mixed Pt 5*d* and 6*p* orbitals with Si 3*p* orbital are responsible for enhanced density of states 1.8 eV below Fermi level. The contribution from Si 3*s* and 3*d* orbitals is rather negligible. Only Pt 5*d*

and Si 3*p* levels contribute to the peak of DOS observed at the energy of −0.8 eV. In the conduction band a well reproduced peak, located at 1.0 eV above Fermi level, is associated with mainly Si 3*d* and 3*s* orbitals, but for the latter in a lower extent. The origin of the peak positioned at 0.2 eV above the Fermi level is not very clear, but it may arise from the surface contribution or from the Si 4*s* orbitals and Pt 5*d* tails from neighboring sites. Although the observed in our experiment DOS reflects reasonably the previously published theoretical predictions,[15,16,48] further surface state sensitive experiments supported by a theoretical approach, including broken symmetry at the surface as well as an alignment of reconstruction atoms, are necessary to understand fully the electronic structure of thin PtSi films.

V. CONCLUSIONS

The growth of platinum silicide by solid state epitaxy reaction, proceeding upon annealing in the wide range of temperatures, has been studied by a scanning tunneling microscopy. For both Pt coverages of 5 ML and 10 ML platinum silicide displays a tendency to form islands with increasing temperature as a result of nonhomogeneous reactions arising from relatively low eutectic point. The size of islands and their distribution depend on the amount of deposited material. The PtSi phase persists from 400 °C up to 750 °C and 950 °C for the coverage of 5 ML and 10 ML, respectively. The orientations of platinum silicide crystallites depend on the amount of initially deposited metal: (010) and (100) planes of PtSi are parallel to Si (111) for 5 ML and 10 ML of Pt, respectively. The variety in the growth mode may result from the multistep thermal treatment procedure of carried experiment. The observed reconstructions terminating PtSi phase have not been reported, yet. The simple models explaining their structure, based only on geometrical relations, were proposed. Their agreement with observed by STM patterns is highly satisfactory. In the case of smaller amount of deposited platinum the periodicity of observed reconstruction is large. The surface, terminated in such way, may serve as a template for a self-organized layer of molecules with diameter up to 2 nm and for catalysis purposes. The measurements of tunneling spectroscopy revealed the character of PtSi as a poor metal with relatively low DOS at the Fermi level. Visible peaks were partially identified as a tails of bulk-like states, supporting recently published theoretical calculations. They originate from strong mixing of Pt and Si orbitals in PtSi compound.

ACKNOWLEDGMENTS

This work was partially supported by the State Committee for Scientific Research (Poland) under Project No. R-48 and by the Grants-in-Aid for Scientific Research from the Ministry of Education, Culture, Sports, Science and Technology in Japan.

*Corresponding author. Email address: wawro@ifpan.edu.pl

[1] E. H. Rhoderick and R. H. Williams, *Metal-Semiconductor Contacts* (Oxford University, Oxford, 1988), p. 201.
[2] M. Wittmer, Phys. Rev. B **43**, 4385 (1991).
[3] J. R. Jimenez, X. Xiao, J. C. Sturm, and P. W. Pellegrini, Appl. Phys. Lett. **67**, 506 (1995).
[4] S. Crattopadhyay, L. K. Bera, C. K. Maiti, S. K. Ray, P. K. Bose, D. Dentel, L. Kubler, and J. L. Bischoff, J. Mater. Sci. **9**, 403 (1998).
[5] K. L. Kavanagh, M. C. Reuter, and R. M. Tromp, J. Cryst. Growth **173**, 393 (1997).
[6] C. Schwarz and H. von Känel, J. Appl. Phys. **79**, 8798 (1996).
[7] D. Drouin, J. Beauvais, R. Lemire, E. Lavallèe, R. Gauvin, and M. Caron, Appl. Phys. Lett. **70**, 3020 (1997).
[8] T. Ohguro, S. Nakamura, M. Koike, T. Morimoto, A. Nishiyama, Y. Ushiku, T. Yoshitomi, M. Ono, M. Saito, and H. Iwai, IEEE Trans. Electron Devices **41**, 2305 (1994).
[9] C. Blair, E. Demirlioglu, E. Yoon, and J. Pierce, Mater. Res. Soc. Symp. Proc. **320**, 53 (1994).
[10] D. X. Xu, J. P. McCaffrey, S. R. Das, G. C. Aers, and L. E. Erickson, Appl. Phys. Lett. **68**, 3588 (1996).
[11] D. M. Solina, R. W. Cheary, P. D. Swift, S. Dligatch, G. M. McCredie, B. Gong, and P. Lynch, Thin Solid Films **372**, 94 (2000).
[12] P. Morgen and B. Jørgensen, Surf. Sci. **208**, 306 (1989).
[13] P. Morgen, M. Szymoński, J. Onsgaard, B. Jørgensen, and G. Rossi, Surf. Sci. **197**, 347 (1988).
[14] D. S. Choi, J. W. Jung, D. S. Shin, M. S. Yoon, W. S. Cho, J. Y. Kim, K. H. Chae, K. H. Jeong, and C. N. Whang, Surf. Sci. **505**, L222 (2002).
[15] N. Franco, J. E. Klepeis, C. Bostedt, T. Van Buuren, C. Heske, O. Pankratov, and L. J. Terminello, J. Electron Spectrosc. Relat. Phenom. **114–116**, 1191 (2001).
[16] N. Franco, J. E. Klepeis, C. Bostedt, T. Van Buuren, C. Heske, O. Pankratov, T. A. Callcott, D. L. Ederer, and L. J. Terminello, Phys. Rev. B **68**, 045116 (2003).
[17] G. Rossi, I. Abbati, L. Braicovich, I. Lindau, and W. E. Spicer, Phys. Rev. B **25**, 3627 (1982).
[18] G. Rossi, D. Chandesris, P. Roubin, and J. Lecante, Phys. Rev. B **34**, R7455 (1986).
[19] J. R. Chen, T. S. Heh, and M. P. Lin, Surf. Sci. **162**, 657 (1985).
[20] L. Ley, Y. Wang, V. Nguyen Van, S. Fisson, D. Souche, G. Vuye, and J. Rivory, Thin Solid Films **270**, 561 (1995).
[21] S. J. Morgan, R. H. Williams, and J. M. Mooney, Appl. Surf. Sci. **56–58**, 493 (1992).
[22] R. A. Donaton, S. Jin, H. Bender, T. Conrad, I. De Wolf, K. Maex, A. Vantomme, and G. Langouche, Electrochem. Solid-State Lett. **2**, 195 (1999).
[23] H. Itoh, S. Narui, A. Sayama, and T. Ichinokawa, Phys. Rev. B **45**, 11136 (1992).
[24] K. Konuma and H. Utsumi, J. Appl. Phys. **76**, 2181 (1994).
[25] G. W. Rubloff, Phys. Rev. B **25**, R4307 (1982).
[26] S. Yamauchi, S. Kawamoto, M. Hirai, M. Kusaka, M. Iwami, H. Nakamura, H. Ohshima, and T. Hattori, Phys. Rev. B **50**, 11564

(1994).
[27] Y. M. Yarmoshenko, S. N. Shamin, L. V. Elokhina, V. E. Dolgih, E. Z. Kurmaev, S. Bartkowski, M. Neumann, D. L. Ederer, K. Göransson, B. Noläng, and I. Engström, J. Phys.: Condens. Matter **9**, 9403 (1997).
[28] M. C. Li, X. C. Chen, W. Cai, J. Yin, J. Yang, G. Wu, and L. Zhao, Mater. Chem. Phys. **72**, 85 (2001).
[29] G. Larrieu, E. Dubois, X. Wallart, X. Baie, and J. Kątcki, J. Appl. Phys. **94**, 7801 (2003).
[30] J. Naftel, I. Coulthard, T. K. Sham, D. X. Xu, L. Erickson, and S. R. Das, Thin Solid Films **308–309**, 580 (1997).
[31] H. Takai, P. A. Psaras, and K. N. Tu, J. Appl. Phys. **58**, 4165 (1985).
[32] R. W. Fathauer, Q. F. Xiao, S. Hashimoto, and C. W. Nieh, Appl. Phys. Lett. **57**, 686 (1990).
[33] J. Y. Tsai, B. Y. Tsui, and M. C. Chen, J. Appl. Phys. **67**, 3530 (1990).
[34] S. M. Zhou, M. Hundhausen, T. Stark, L. Y. Chen, and L. Ley, J. Vac. Sci. Technol. A **17**, 144 (1999).
[35] T. Stark, H. Grünleitner, M. Hundhausen, and L. Ley, Thin Solid Films **358**, 73 (2000).
[36] A. Rahman, C. W. Bates Jr., W. P. Lowe, and A. F. Marshall, Mater. Sci. Eng., B **77**, 241 (2000).
[37] A. J. Nelson, M. Danailov, A. Barinov, B. Kaulich, L. Gregoratti, and M. Kiskinova, Appl. Phys. Lett. **81**, 3981 (2002).
[38] J. E. McLeod, M. A. E. Wandt, R. Pretorius, and C. M. Comrie, J. Appl. Phys. **72**, 2232 (1992).
[39] C. C. Tsai, R. J. Nemanich, and T. W. Sigmon, J. Phys. Soc. Jpn. **49**, 1265 (1980).
[40] C. A. Crider and J. M. Poate, Appl. Phys. Lett. **36**, 417 (1980).
[41] F. Nava, S. Valeri, G. Majni, A. Cembali, G. Pignatel, and G. Queirolo, J. Appl. Phys. **52**, 6641 (1981).
[42] C. A. Crider, J. M. Poate, J. E. Rowe, and T. T. Sheng, J. Appl. Phys. **52**, 2860 (1981).
[43] S. M. Goodnick, M. Fathipour, D. L. Ellsworth, and C. W. Wilmsen, J. Vac. Sci. Technol. **18**, 949 (1981).
[44] S. Mantovani, F. Nava, C. Nobili, and G. Ottaviani, Phys. Rev. B **33**, 5536 (1986).
[45] S. Okada, Y. Kishikawa, K. Oura, and T. Hanawa, Surf. Sci. **100**, L457 (1980).
[46] W. S. Yang, S. C. Wu, and F. Jona, Surf. Sci. **169**, 383 (1986).
[47] J. E. Klepeis, O. Beckstein, O. Pankratov, and G. L. W. Hart, Phys. Rev. B **64**, 155110 (2001).
[48] O. Beckstein, J. E. Klepeis, G. L. W. Hart, and O. Pankratov, Phys. Rev. B **63**, 134112 (2001).
[49] A. K. Sinha, R. B. Marcus, T. T. Sheng, and S. E. Haszko, J. Appl. Phys. **43**, 3637 (1972).